Proceedings of the 2001 Particle Accelerator Conference, Chicago

PROTECTING LHC COMPONENTS AGAINST RADIATION RESULTING FROM AN UNSYNCHRONIZED BEAM ABORT*

N.V. Mokhov†, A.I. Drozhdin, I.L. Rakhno, FNAL, Batavia, IL 60510, USA
M. Gyr, E. Weisse, CERN, Geneva, CH-1211, Switzerland

Abstract

The effect of possible accidental beam loss in the LHC on the IP5 and IP6 insertion elements is studied via realistic Monte Carlo simulations. The scenario studied is beam loss due to unsynchronized abort at an accidental prefire of one of the abort kicker modules. Simulations show that this beam loss would result in severe heating of the IP5 and IP6 superconducting (SC) quadrupoles. Contrary to the previous considerations with a stationary set of collimators in IP5, collimators in IP6 close to the cause are proposed: a movable collimator upstream of the Q4 quadrupole and a stationary one upstream of the extraction septum MSD. The calculated temperature rise in the optimal set of collimators is quite acceptable. All SC magnets are protected by these collimators against damage.

1 INTRODUCTION

Each of the two circulating 7 TeV proton beams of the Large Hadron Collider (LHC) [1] will contain nominally 350 MJ of energy. An accidental beam loss caused by an unsynchronized abort or abort system trigger malfunction, can cause severe damage to the collider equipment. Such a malfunction can be initiated, *e.g.*, by a high energy cosmic particle crossing a sensitive element of the trigger. The process is shown schematically in Fig. 1. A prefired kicker module induces coherent beam oscillations with an amplitude up to 21σ of the beam at collision. Simulations show that if this happens at the top energy, starting from 70-80% of the kicker strength, the misbehaved beam ends up in the IP5 inner triplet causing destruction of its components [2]. To avoid this, the other kicker modules are fired immediately after (unsynchronized abort), but this does not prevent beam loss completely. At normal operation the kicker front is placed in a longitudinal gap in the circulating beam to prevent particle loss during the rise of the kicker pulse. At the unsynchronized abort the kicker front does not coincide with this gap. As a result, it causes beam loss at the collider limiting aperture. A set of stationary shadow collimators for the IP5 outer triplet has been proposed in Ref. [2] to protect the LHC machine against irreversible consequences of fast beam loss. Here we propose a set of movable collimators in the IP6 region as close to the cause as possible.

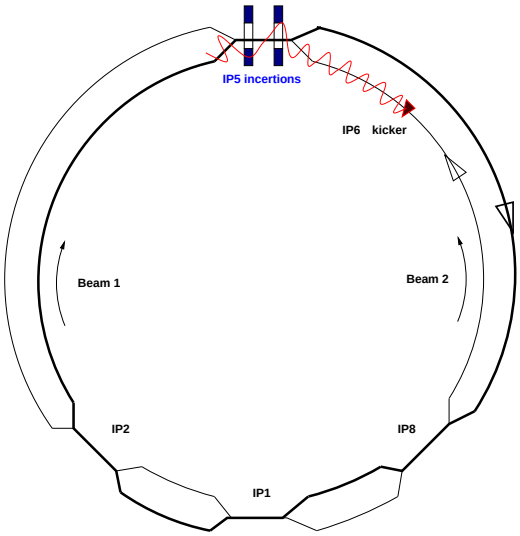

Figure 1: LHC abort kicker prefire.

2 MODELING IN IP5 AND IP6

A new detailed calculation model was developed based on the current LHC lattice (version 6.2), latest advanced version of the MARS14 code system [3], and upgraded STRUCT code [4]. A calculational model of a 380-m long section of IP6—from the region upstream of the MSD septum through SC Q4, Q5 and Q8 quadrupoles and first four MB magnets—was built, its fraction is shown in Fig. 2.

To protect the lattice elements against overheating at unsynchronized abort, movable shadow collimators (TCDQ) are placed close to the beam upstream of the Q4 quad in IP6. The system considered at this stage includes a set of graphite/aluminum jaws aligned with the envelope of the circulating beam (see Fig. 3). The jaws are retracted to about 20-25 mm at injection and positioned at 9 mm at collision from the closed orbit in a horizontal plane. The tracking in the IP6-IP5 octant, performed with such collimators in, shows no beam loss in the IP5 inner triplet. A stationary collimator (TCDS) is used to protect the extraction septum magnet MSD, which consists of 15 modules in the region of the center of IP6. A rectangular graphite module 5 m long and 23 mm wide is considered at present. Overlapped cross sections of the collimator and the first of the MSD modules are presented in Fig. 4. The results below are given for a 20-mm wide (rather than 23 mm) collimator, positioned at 0.5 mm from the right edge of the septum gap. Other options for TCDS length, shape, and position relative to the septum magnet are under investigation.

* Work supported by the Universities Research Association, Inc., under contract DE-AC02-76CH03000 with the U.S. Department of Energy.
† mokhov@fnal.gov

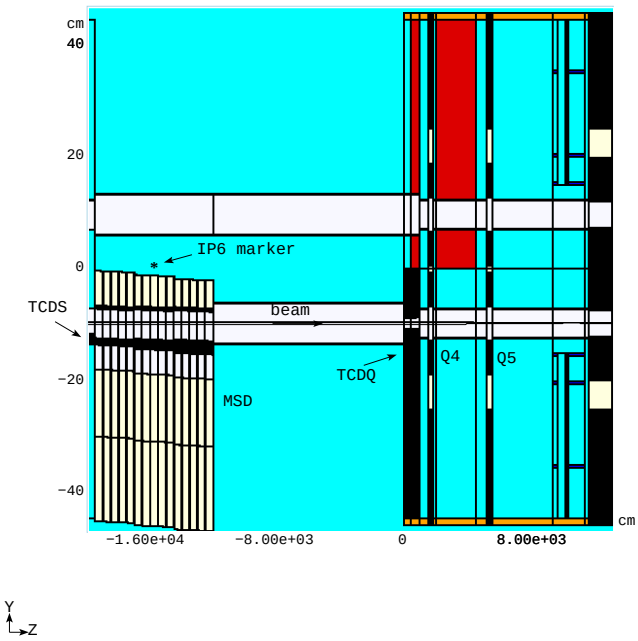

Figure 2: Central part of the IP6 MARS model.

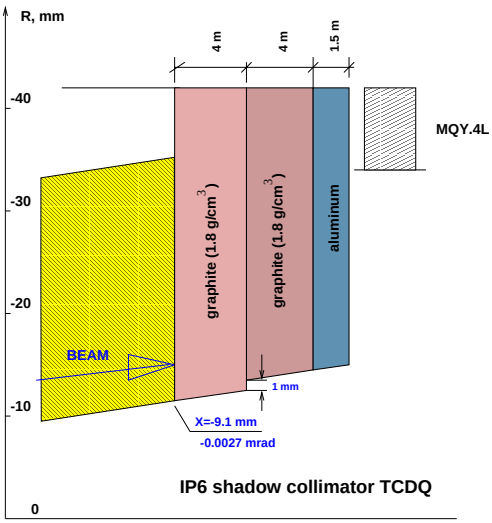

Figure 3: TCDQ graphite/aluminum collimator before Q4.

Simulating beam loss during the kicker rise time, we assume a uniform beam distribution around the LHC with a 24.95 ns bunch separation with an abort gap of 3 μs, corresponding to the kicker rise time. If one of the 14 abort kicker modules prefires, the other 13 modules are fired within the next microseconds to extract the beam. In calculations every bunch is affected by the abort kicker with gradually increasing strength. Three delay intervals between the kicker prefire and firing the other kickers are considered: 1.2, 3.0, and 4.0 μs. The present design aims to obtain the lowest one. In all cases not more than 280 bunches (corresponding to 7 μs) are affected.

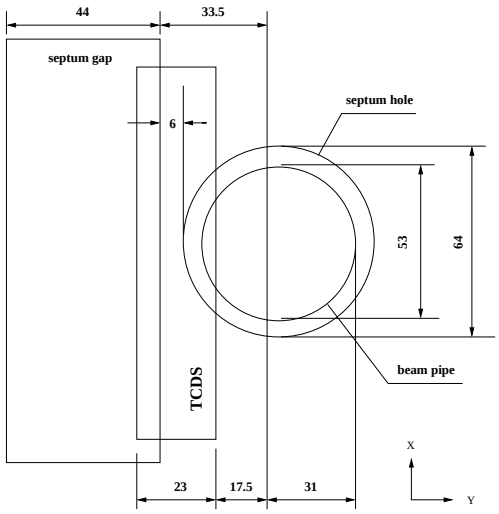

Figure 4: Graphite collimator TCDS to protect extraction septum magnet MSD (all dimensions are in mm).

3 RESULTS AND DISCUSSION

3.1 Temperature Rise

To find the maximum energy deposition in each element, the TCDS and TCDQ collimators, MSD septum magnet and superconducting coils were subdivided into a large number of cells according to the calculated beam distribution at their upstream ends. The MSD modules were subdivided into five 6×6 mm^2 longitudinal regions each, with one layer horizontally in MSD-1 through MSD-5, two in MSD-6 through MSD-10, and three in MSD-11 through MSD-15. Instantaneous temperature rises, given in Table 1, refer to the maxima in such $6\times6\times890$ mm^3 cells for the representative modules. Statistical uncertainties (hereinafter 1σ) are equal to 3% for TCDS and TCDQ-1 and 10% for MSD-1 and TCDQ-2. One can conclude from the Table that neither of the collimators under investigation will be melted down. At the same time heating of the warm magnet MSD will not exceed 100 degrees which ensures its stable operation.

Table 1: Peak local temperature rise ΔT (C) for the collimators and some of the IP6 MSD modules

Module	Delay time (μs)		
	1.2	3.0	4.0
TCDS	470	487	490
MSD-1	88	92	84
MSD-6	6.5	7.0	6.5
MSD-11	1.0	1.0	0.8
MSD-15	0.07	0.07	0.12
TCDQ-1 (4 m)	455	810	1200
TCDQ-2 (4 m)	157	250	336
TCDQ-3 (1.5 m)	5	17	38

3.2 *Integral Energy Deposition*

When considering both cryogenic and non-cryogenic equipment, total energy deposition over its volume is of a great practical interest. Table 2 shows total energy deposition in the collimators, MSD modules, and several SC magnets downstream of the IP6 marker. For the magnets, the "total energy" includes energy deposited in SC coils themselves as well as in beam screens, coolant (He) *etc.* up to the steel vessel (but excluding the latter) which separates the cold mass from the warm surroundings. Calculated statistical uncertainty for the last row in the Table is about 30%.

The peak temperatures in the TCDS collimator and first of the MSD modules differ significantly (see Table 1) while total energies deposited are comparable. It means that the collimator provides nice protection and a substantial amount of energy contained in the beam is deposited over the bulky MSD module instead of the septum-magnet septa 6-mm thick (see Fig. 4) where the peak temperature is calculated.

Table 2: Total energy deposition ΔE (kJ) in IP6 components

Module	Relative position*) (m)	Delay time (μs)		
		1.2	3.0	4.0
TCDS	-42.1	929	970	961
MSD-1	-36.6	1270	1330	1310
MSD-6	-12.05	35	43	41
MSD-11	12.5	14	17	21
MSD-15	32.14	5	5	6
TCDQ-1	155.3	1540	2450	3420
TCDQ-2	159.3	542	1020	1640
TCDQ-3	160.8	64	151	318
Q4	170.1	25	92	260
Q5	206.5	5.4	24	77
MBA-1	270.1	3.0	17	58
MBB-1	285.8	0.3	2.3	7.5
Q8	302.1	0.02	0.4	1.0
MBA-2	309.2	0.11	0.5	2.1
MBB-2	324.8	0.04	0.4	1.8

*) Between upstream end and IP6 marker.

3.3 *Peak Energy Deposition in Cold Magnets*

For SC coils more detailed data are usually required which, among other things, enable to determine whether it will quench or not. Energy deposition density distributions were calculated in the IP6 SC Q4, Q5 and Q8 quadrupoles and MBA-1, MBB-1, MBA-2 and MBB-2 dipoles. The peak energy deposition density ϵ_{max} in the SC coils should be compared to the quench limit that can be estimated as 0.5 mJ/g per pulse for the LHC magnets at fast beam loss ($\leq$20 μs) [5]. The values of calculated ϵ_{max} in the considered seven SC magnets are presented in Fig. 5, with the word "peak" referring to the highest value over length of each magnet. The first points are statistically valid within 5-10%, while the last ones are obtained with poorer statistics. One can conclude that no SC coils in the LHC will be damaged at an unsynchronized abort for the delay times considered. At the same time, the first seven SC magnets downstream of IP6 will be subject to quench.

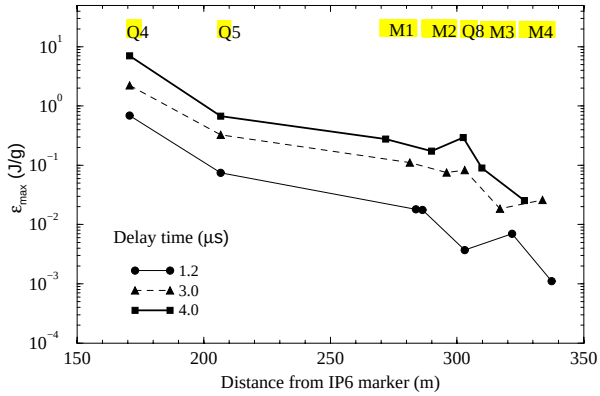

Figure 5: Distribution of peak energy deposition density ϵ_{max} in SC magnets *vs.* distance from IP6, where M1 *etc.* denote the first four dipoles in the region (see Table 2).

4 CONCLUSIONS

The proposed protection system will reliably protect the machine components at an unsynchronized abort in the LHC IP6. The study performed revealed that with this system, the peak temperature rise in all the IP6 components is quite acceptable. All the LHC SC dipoles and quadrupoles are protected against damage in such an accidental event. At the same time, the first seven to ten SC magnets after IP6 are subject to quench at unsynchronized abort, even for the lowest delay time considered (1.2 μs). Additional calculational and engineering studies are required for the proposed system to reduce energy deposition in the magnets.

5 REFERENCES

[1] The Large Hadron Collider Conceptual Design, CERN/AC/95-05(LHC), 1995, P. Lefèvre and T. Pettersson, editors.

[2] A.I. Drozhdin, N.V. Mokhov, M. Huhtinen, Proc. of the 1999 Part. Accel. Conf., New York, 1999, p. 1231.

[3] N. V. Mokhov, "The MARS Code System User's Guide", Fermilab-FN-628 (1995); N. V. Mokhov and O. E. Krivosheev, "MARS Code Status", Fermilab-Conf-00/181 (2000). http://www-ap.fnal.gov/MARS/.

[4] I. S. Baishev, A. I. Drozhdin and N. V. Mokhov, "STRUCT Program User's Reference Manual", SSCL–MAN–0034 (1994); http://www-ap.fnal.gov/∼drozhdin/.

[5] Fermilab Superconducting Accelerator Design Report, Fermilab, 1979.